

# Doping Dependence of the Pseudogap State in the ab-plane IR Response of $\text{La}_{2-x}\text{Sr}_x\text{CuO}_4$

T. Startseva<sup>(1)</sup>, T. Timusk<sup>(1)</sup>, A. V. Puchkov<sup>(2)</sup>, D. N. Basov<sup>(3)</sup>, H. A. Mook<sup>(4)</sup>, T. Kikura<sup>(5)</sup>, and K. Kishio<sup>(5)</sup>

<sup>(1)</sup> Department of Physics and Astronomy, McMaster University  
Hamilton, Ontario, CANADA L8S 4M1

<sup>(2)</sup> Department of Applied Physics, Stanford University, Stanford, CA 94305

<sup>(3)</sup> Department of Physics, University of California San-Diego, La Jolla, CA 92093

<sup>(4)</sup> Oak Ridge National Laboratory, Oak Ridge, Tennessee 37831

<sup>(5)</sup> Department of Applied Chemistry, University of Tokyo, Tokyo 113, Japan  
(June 10, 1997, submitted to Phys. Rev. B)

The ab-plane optical spectra of two single crystals of  $\text{La}_{2-x}\text{Sr}_x\text{CuO}_4$ , one underdoped and one overdoped were investigated. We observe a gap-like depression of the effective scattering rate  $1= (\hbar/T)$  below  $700 \text{ cm}^{-1}$  in both systems. This feature persists up to 300 K in the underdoped sample with the concentration of  $\text{Sr } x = 0.14$  but loses prominence at temperatures above 300 K in the overdoped regime ( $x = 0.22$ ). Below  $700 \text{ cm}^{-1}$   $1= (\hbar/T)$  is temperature dependent and superlinear in frequency for both samples. Above this frequency the effective scattering rate becomes linear in frequency and is temperature independent in the case of the underdoped  $\text{La}_{1.86}\text{Sr}_{0.14}\text{CuO}_4$  up to 300 K. On the other hand, the overdoped  $\text{La}_{1.78}\text{Sr}_{0.22}\text{CuO}_4$  shows a  $1= (\hbar/T)$  temperature dependence above  $700 \text{ cm}^{-1}$  at all temperatures. This behaviour of the frequency and temperature dependent scattering rates is a signature of a pseudogap state in other materials and suggests that both the under and overdoped single-layer HTSC systems  $\text{La}_{2-x}\text{Sr}_x\text{CuO}_4$  have a pseudogap at temperatures exceeding 300 K.

Right from the discovery of high-temperature superconductivity (HTSC) in the complex copper oxides, it has been recognized that the  $\text{CuO}_2$  planes play an important role in the nature of this phenomenon. While all of the cuprates share this structural element,  $\text{La}_{2-x}\text{Sr}_x\text{CuO}_4$  (LSCO) possesses only one  $\text{CuO}_2$  plane per unit cell which makes it an excellent prototype system for examining the role played by the  $\text{CuO}_2$  planes. It is also a good model for the study of doping dependence since it can be doped by the addition of strontium over a wide range: from the underdoped, where  $T_c$  increases with Sr content, to the optimally doped where  $T_c$  reaches its maximum value of  $\sim 40 \text{ K}$ , and to the overdoped region where  $T_c \rightarrow 0$  at  $x = 0.34$ .<sup>1</sup>

It is well known that the in-plane transport properties of HTSC materials are anomalous. For example, the in-plane dc resistivity,  $\rho_{ab}(T)$ , for the samples doped close to the optimal doping level, is linear in temperature from the superconducting transition temperature  $T_c$  to well above 900 K. At the same time, underdoped samples show a crossover from the linear  $T$  dependence to a superlinear,  $\rho_{ab}(T) = T^{1+\alpha}$ , below a characteristic temperature  $T^*$ . It was shown by B. Batlogg et al.<sup>1</sup> that  $T^*$  decreases from 800 K to approximately 300 K as the doping level is increased from the strongly underdoped to just over the optimal doping level. Similar behavior at  $T = T^*$  has been observed in the Hall effect coefficient and the magnetic susceptibility.<sup>2,3</sup>

A completely satisfactory microscopic understanding of the peculiar transport properties of HTSC is missing at this time. However, the temperature and doping de-

pendences of the crossover behaviour at  $T = T^*$  noted in the dc transport properties are in accord with the idea that a pseudogap forms in the spectrum of the low-energy electronic excitations responsible for the scattering of the charge carriers. A similar gap-like feature has been observed experimentally in the nuclear magnetic resonance (NMR)<sup>4</sup>, the angular resolved photoemission (ARPES)<sup>5</sup>, specific heat and the infrared optical<sup>7,9</sup> (IR) measurements. All of these observations can be consistently interpreted in terms of a pseudogap. In this picture the dc transport properties and the gap formation are intimately related: a gap in the density of states near the Fermi level will result in a reduced  $1= (\hbar/T)$  in the temperature and spectral region where this gap occurs. Since the ARPES results suggest that the gap has a  $d_{x^2-y^2}$  momentum dependence, momentum-averaging measurement techniques, like NMR or IR optical, would observe a pseudogap rather than a full gap even at lowest temperatures where this gap is fully formed.

A pseudogap feature was observed in the c-axis IR conductivity in  $\text{YBa}_2\text{Cu}_3\text{O}_{7-x}$  (Y123) and  $\text{YBa}_2\text{Cu}_4\text{O}_8$  (Y124) materials.<sup>7,10</sup> The ab-plane results show increased coherence (a narrower Drude peak) upon entering the pseudogap state while the c-axis optical response shows a depressed conductivity. The pseudogap state is seen in both the c-axis conductivity and the ab-plane scattering rate in the same doping and temperature region, suggesting that the two phenomena are closely related.<sup>7</sup> Recent c-axis optical results on single crystals of slightly underdoped  $\text{La}_{1.86}\text{Sr}_{0.14}\text{CuO}_4$ <sup>11</sup> show that the pseudogap state in the c-axis direction of this material is not as well

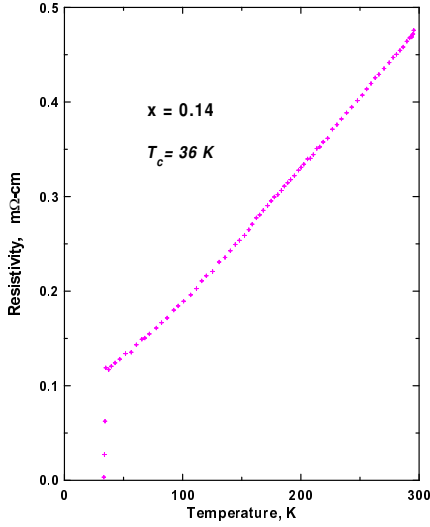


FIG. 1. The temperature dependence of the in-plane resistivity of  $\text{La}_{1.86}\text{Sr}_{0.14}\text{CuO}_4$  is shown with a sharp superconducting transition at 36 K. The shape of the curve is consistent with  $T_c$  being greater than 300 K.

defined as it is in the two plane materials. However, as the doping is reduced further the c-axis pseudogap state features become clearer below 0.1 eV.<sup>12</sup>

The weak pseudogap as seen by NMR and neutron scattering<sup>13</sup> in LSCO has led to the suggestion that the existence of the pseudogap in the spin excitation spectrum is only possible in bilayer compounds such as Y123 and Y124. In particular, Millis and Monien attribute the pseudogap (or the spin gap) to strong antiferromagnetic correlations between the planes in the bilayer, which are responsible for a quantum order-disorder transition.<sup>4</sup> However, the characteristic deviations below the linear extrapolation and  $T^*$  seen in dc conductivity in the bilayer materials<sup>14</sup> are also seen in LSCO.<sup>14</sup> Thus, it is important to see if the characteristic depression of the frequency dependent scattering rate in the pseudogap state, seen in the bilayer materials<sup>7,9</sup>, can also be observed in the single plane materials such as LSCO.

Previous work on the inplane far infrared optical properties of the single layer lanthanum strontium cuprate includes work on the oxygen doped  $\text{La}_2\text{CuO}_4$ <sup>15</sup>, thin films of LSCO<sup>16</sup> as well as single crystal work at room temperature<sup>14</sup>. To our knowledge, a study of the temperature and doping dependence has not been done. We fill this gap here by performing optical measurements on high-quality LSCO single crystals at temperatures ranging from 10 K to 300 K at two different doping levels.

To better display the effect of increased coherence resulting from the formation of the pseudogap state, a memory function, or extended Drude analysis is used.

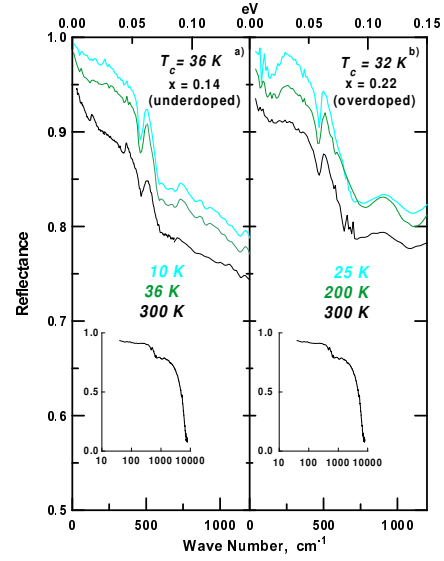


FIG. 2. The reflectance of  $\text{La}_{1.86}\text{Sr}_{0.14}\text{CuO}_4$  (a) and  $\text{La}_{1.78}\text{Sr}_{0.22}\text{CuO}_4$  (b) is shown at three temperatures: 10 K, 36 K and 300 K. The thickness of the line goes up as the temperature goes down. Phonon peaks are visible at 150, 300 and 500  $\text{cm}^{-1}$ . The insert in the left panel is a semi-log graph of the reflectance at 300 K which shows a plasma edge around 7000  $\text{cm}^{-1}$ .

In this treatment the complex optical conductivity is modeled by a Drude peak with a frequency-dependent scattering rate and an effective electron mass.<sup>17,18</sup> While the optical conductivity tends to emphasize free particle behaviour, a study of the frequency dependence of the effective scattering rate puts more weight on displaying the interactions of the free particles with the elementary excitations of the system.<sup>19</sup> The temperature evolution of the frequency dependent scattering rate and effective mass spectra are of particular interest and are defined as follows:

$$1 = \langle \sigma \rangle(T) = \frac{\omega_p^2}{4} \text{Re} \left( \frac{1}{\langle \sigma \rangle(T)} \right) \quad (1)$$

$$\frac{m}{m_e} \langle \sigma \rangle(T) = \frac{1}{4} \frac{\omega_p^2}{\langle \sigma \rangle(T)} \text{Im} \left( \frac{1}{\langle \sigma \rangle(T)} \right) \quad (2)$$

Here,  $\langle \sigma \rangle(T) = \sigma_1(\omega; T) + i \sigma_2(\omega; T)$  is the complex optical conductivity and  $\omega_p$  is the plasma frequency of charge carriers.

The single crystals of  $\text{La}_{2-x}\text{Sr}_x\text{CuO}_4$  with approximate dimensions  $5 \times 3 \times 3 \text{ mm}^3$  were grown by the travelling-solvent coating zone technique at Oak Ridge<sup>20</sup> in the case of  $x = 0.14$  and in Tokyo<sup>21</sup> in the case of  $x = 0.22$ . The critical temperature was determined by both SQUID magnetization and resistivity measurements.

and was found to be 36 K for the nominal concentration of  $\text{Sr } x = 0.14$  and 32 K for  $x = 0.22$ . Since the highest  $T_c$  in the LSCO system has been found at to be 40 K  $x = 0.17$ , we conclude that the  $x = 0.14$  crystal is underdoped and the  $x = 0.22$  is overdoped. The crystal with  $x = 0.14$  was aligned using Laue diffraction and polished parallel to the  $\text{CuO}_2$  planes. The crystal with  $x = 0.22$  was polished in Tokyo in the direction of the  $ab$ -plane. It is important to have the sample surface accurately parallel to the  $ab$ -plane to avoid any  $c$ -axis contribution to the optical conductivity.<sup>22</sup> The miscut of the sample on the  $ab$ -plane was checked by a high precision triple axis x-ray diffractometer and was determined to be less than 0.8%.

All reflectivity measurements were performed with a Michelson interferometer using three different detectors which cover frequencies ranging from 10 to 10000  $\text{cm}^{-1}$ . The experimental uncertainty in the reflectance data does not exceed 1%. The dc resistivity measurements were carried out using a standard 4-probe technique.

The result of the resistivity measurement on the  $\text{La}_{1.86}\text{Sr}_{0.14}\text{CuO}_4$  single crystal, used in the optical measurements, is shown in Fig. 1. It is commonly accepted that the dc resistivity is linear at high temperatures for LSCO and that the pseudogap begins to form near the temperature where the resistivity drops below this linear trend.<sup>1</sup> At lower temperatures there is a region of superlinear temperature dependent resistivity. The  $T$  value for our samples with  $x = 0.14$  and  $x = 0.22$ , extracted from the phase diagram of Batlogg et al.,<sup>1</sup> are 450 K and 200 K, respectively. In agreement with this, the resistivity shows a superlinear temperature dependence below room temperature as expected in the pseudogap region.

In Fig. 2 we present the reflectivity data at temperatures above and below  $T_c$ . For clarity, only three temperatures are shown:  $T = 300$  K, a temperature just above the superconducting transition and a low temperature

10 K or 25 K for  $x = 0.14$  and  $x = 0.22$ , respectively, in the superconducting state. In the frequency region shown the reflectance is strongly temperature dependent for both materials, dropping by approximately 10% as temperature is increased from the lowest temperature to  $T = 300$  K. The plasma edge is observed at 7800  $\text{cm}^{-1}$  (see insert of Fig. 2). The distinct peaks at approximately 150, 300 and 500  $\text{cm}^{-1}$  in the LSCO reflectivity spectra correspond to the excitation of  $ab$ -plane TO phonons.<sup>23</sup>

The complex optical conductivity  $\sigma(\omega)$  was obtained by Kramers-Kronig analysis of the reflectivity data. Since, in principle, this analysis requires knowledge of the reflectance at all frequencies, reflectivity extensions must be used at high and low frequencies. The Hagen-Rubens formula was used for the low frequency reflectivity extrapolation, with parameters taken from the dc resistivity measurements on the same sample shown in Fig. 1 and the results of H. Takagi et al.<sup>24</sup> for the overdoped sample. For the high-frequency extension with  $\omega > 8000$   $\text{cm}^{-1}$  we used reflectivity results of Uchida et al.<sup>14</sup> At frequencies higher than 40 eV the reflectivity was

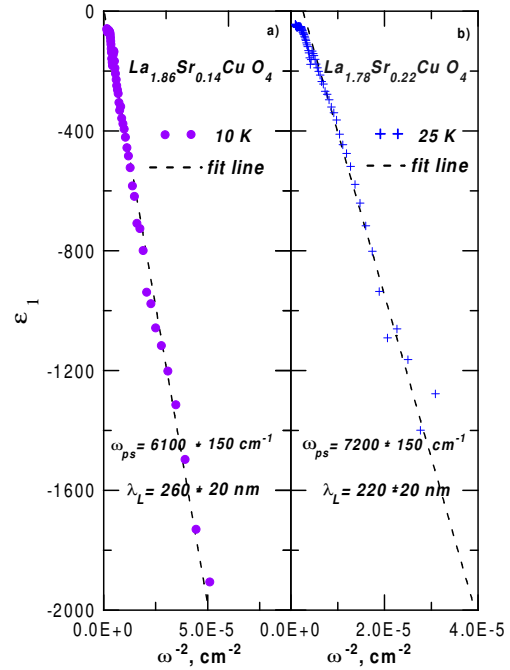


FIG. 3. The real part of the dielectric function as a function of  $\omega^2$  of  $\text{La}_{1.86}\text{Sr}_{0.14}\text{CuO}_4$  at 10 K in the panel a) and of  $\text{La}_{1.78}\text{Sr}_{0.22}\text{CuO}_4$  at 25 K at the panel b). The dash line is linear fit. The slope of the fit gives the values of both a superconducting plasma frequency of LSCO and the London penetration depth.

assumed to fall as  $\omega^{-4}$ .

We calculate the plasma frequency of the superconducting charge carriers and the London penetration depth using the following formula:<sup>26</sup>

$$\epsilon_1 = 1 - \frac{\omega_{ps}^2}{\omega^2} \quad (3)$$

The slope of the low-frequency dielectric function,  $\epsilon_1(\omega)$ , plotted as a function of  $\omega^2$  in Fig. 3a,b gives plasma frequencies of 6100  $\text{cm}^{-1}$  and 7200  $\text{cm}^{-1}$  in the superconducting state. The corresponding London penetration depths are  $\lambda_L = 1/2 \omega_{ps} = 250$  nm and 220 nm for  $\text{La}_{1.86}\text{Sr}_{0.14}\text{CuO}_4$  and  $\text{La}_{1.78}\text{Sr}_{0.22}\text{CuO}_4$ , respectively. These values are in good agreement with those obtained previously by Gao et al. in  $\text{InSb}$  ( $\lambda_L = 275 \pm 5$  nm) and by muon-spin-relaxation<sup>25</sup> ( $\lambda_L = 250$  nm).

The real part of the conductivity for the two materials is shown in Fig. 4a,b. For completeness we also show the imaginary part of the conductivity in Fig. 4c,d. The real part of the conductivity has a Drude peak which narrows as the temperature decreases in agreement with the metallic temperature dependence of the dc resistivity. The conductivity of LSCO is temperature-dependent

in the M IR frequency region as well. This temperature dependence becomes stronger as  $T_c$  is reduced by overdoping. There are strong deviations from the Drude shape in the form of an onset or a step in the conductivity at  $700 \text{ cm}^{-1}$ . Unlike the Y123, Y124, and  $\text{Bi}_2\text{Sr}_2\text{CaCu}_2\text{O}_{8+x}$  (Bi2212) materials which show similar features only at low temperature, the optical conductivity of  $\text{La}_{1.86}\text{Sr}_{0.14}\text{CuO}_4$  shows a threshold at about  $700 \text{ cm}^{-1}$  already at room temperature.

Another deviation from the Drude form is a shift of the Drude peak from zero frequency to  $150 \text{ cm}^{-1}$ . This peak grows in magnitude and narrows as the doping level of Sr increases. A similar peculiarity was observed in the conductivity of a single crystal of  $\text{La}_{2-x}\text{Sr}_x\text{CuO}_4$ <sup>15</sup>; however, it was absent in the optical data of  $\text{La}_{2-x}\text{Sr}_x\text{CuO}_4$  thin films.<sup>16</sup> The nature of the peak is unclear. It is seen in many HTSC systems and has been attributed to localization.<sup>27</sup> An artifact of the polished surface is another possible explanation.

We define an overall plasma frequency in terms of the sum rule  $\omega_p^2 = 8\pi \int_0^{\omega_{\text{max}}} \omega^{-1}(\omega) d\omega$  with  $\omega_{\text{max}} = 8000 \text{ cm}^{-1}$ . At room temperature,  $\omega_p = 15100 \text{ cm}^{-1}$  and  $13800 \text{ cm}^{-1}$  for LSCO with  $x = 0.14$  and  $x = 0.22$ , respectively. These numbers are similar to those measured previously<sup>16,28,15</sup> and were used to calculate the frequency-dependent scattering rate using Eq. 1. In a recent survey on a number of compounds, Puchkov et al.<sup>9</sup> found that while the plasma frequency grows with doping in the underdoped region, this growth stops at optimal doping. In agreement, we observe here a slight drop in the spectral weight as one moves from the slightly underdoped to the overdoped region.

The frequency dependent scattering rate and the effective mass are shown in Fig. 5. The spectra can conveniently be divided into two regions. In the high frequency region, starting at about  $700 \text{ cm}^{-1}$ , the scattering rate varies linearly with frequency while in the low frequency region there is a clear suppression of  $1/(\omega, T)$  below this linear trend. We will call this frequency region of suppressed scattering the pseudogap state region. As the temperature is lowered this suppression becomes deeper. The dashed lines in Fig 5 are extrapolations of the high frequency linear behaviour to zero frequency. A pseudogap state can be defined in terms of this suppression of scattering: the material is in the pseudogap state when the scattering rate falls below the high frequency straight-line extrapolation. In the low frequency limit the scattering rate is proportional to the dc resistivity. Due to this, the  $1/(\omega, T)$  suppression should be compared to the suppression of  $\rho_{\text{dc}}(T)$ <sup>1</sup> at temperatures below the linear  $T$  dependence region. The IR measurement gives us the possibility to see both the frequency and the temperature dependence of this feature.

The temperature dependence above  $700 \text{ cm}^{-1}$  is strongly influenced by the level of Sr doping. In the underdoped sample the high frequency scattering rate is nearly temperature independent. In contrast, the over-

doped samples scattering rate above  $700 \text{ cm}^{-1}$  increases uniformly with temperature. The curves are seen to be displaced parallel to each other as the temperature is increased. This behaviour is also seen in other overdoped HTSC.<sup>29</sup>

To emphasize the difference between the underdoped and overdoped regimes we fitted the high frequency scattering rate curves with a linear function  $\frac{1}{(\omega)} = \omega + \omega_0$ . The values of the  $\omega_0$  parameters can be found in Table 1. The zero-frequency intercept,  $\omega_0$ , changes only by 7% in the case of underdoped sample but nearly doubles in the overdoped sample between the superconducting transition and  $300 \text{ K}$ . While  $\omega_0$  increases with doping,  $\omega_0$  is substantially smaller in the overdoped sample. The behavior of the intercept is consistent with the other HTSC materials<sup>29</sup> but not the slope. Puchkov et al. found that  $\omega_0$  decreased with doping in most materials. The magnitudes of  $\omega_0$  and  $\omega_p$  of LSCO seem to be substantially lower than those of Y123, Y124, Bi2212 and Tl2202.<sup>29</sup>

We found that for  $\text{La}_{1.78}\text{Sr}_{0.22}\text{CuO}_4$  (the overdoped sample)  $T^*$  ( $\approx 300 \text{ K}$ ) is an order of magnitude higher than the superconducting transition temperature  $T_c$  ( $32 \text{ K}$ ). This is significantly different than previous results on overdoped cuprates. Theoretical considerations have led to the suggestion that  $T^*$  coincides with the temperature of the superconducting transition at the optimal doping level.<sup>30,31</sup> This seems to apply to Y123 and Y124 where the  $T^*$  and  $T_c$  curves cross near the optimal doping level, but this is clearly not the case here. A detailed examination of the scattering rate curves in Fig. 5b suggests that in overdoped sample the suppression of the scattering disappears near room temperature implying that  $T^*$  for  $x = 0.22$  is close to  $300 \text{ K}$ . This result is consistent with the phase diagram based on the data from transport properties.<sup>1</sup>

In addition to the pseudogap depth and temperature dependence, several other features of Figs. 5 a,b should be mentioned. The position of the pseudogap remains at  $700 \text{ cm}^{-1}$  for all temperatures. There are also several peaks positioned at  $1000 \text{ cm}^{-1}$  in scattering rate which complicate the analysis, particularly in the case of the overdoped samples. These peaks have been attributed to polaronic effects.<sup>32,33</sup>

For completeness we plot the effective mass of underdoped sample (Fig. 5c) and the overdoped sample (Fig. 5d). As expected,  $\frac{m^*(\omega)}{m_e}$  rises to a maximum value between 2 and 5 in the region of the scattering rate suppression. The enhancement of the effective mass in the pseudogap state as well as the upper limit of  $\frac{m^*(\omega)}{m_e}$  are similar to what has been previously reported for values Y123, Y124 and Bi2212.<sup>29</sup>

Before closing we compare our results with data of Gao et al.<sup>16</sup> on  $\text{La}_{2-x}\text{Sr}_x\text{CuO}_{4+\delta}$  films and Quijada et al.<sup>15</sup> on oxygen doped  $\text{La}_2\text{CuO}_{4+\delta}$ . Our results in the underdoped case are comparable with those of the oxygen doped material, although Quijada et al. did not carry out

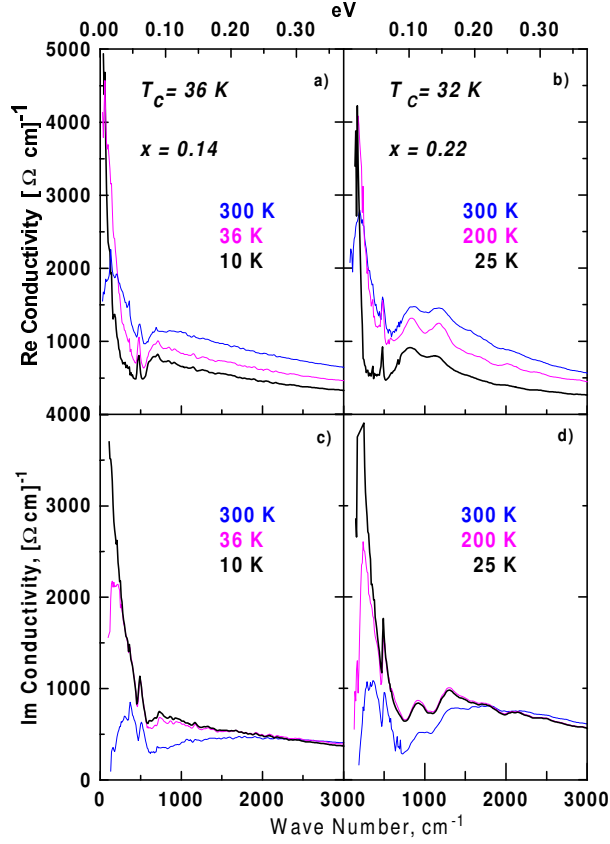


FIG. 4. The temperature dependence of the in-plane conductivity of underdoped  $\text{La}_{1.86}\text{Sr}_{0.14}\text{CuO}_4$  (left panel) and overdoped  $\text{La}_{1.78}\text{Sr}_{0.22}\text{CuO}_4$  (right panel) are shown. The real part of conductivity (a,b) is suppressed below  $700\text{ cm}^{-1}$ . The Drude-like peak forms at room temperature and narrows as  $T$  decreases. The imaginary part of the conductivity is shown on the lower panel (c,d). Thin line is room temperature and thick line represents a temperature below superconducting transition.

TABLE I. Linear fit parameters to the scattering rate of  $\text{La}_{2-x}\text{Sr}_x\text{CuO}_4$

Sr content	$T_c$	$T$		
$x = 0.14$	36 K	300 K	0.32	1578
		36 K	0.44	1467
		10 K	0.44	1467
$x = 0.22$	32 K	300 K	0.39	1260
		200 K	0.5	828
		25 K	0.61	721

a frequency dependent scattering rate analysis for their underdoped sample. The  $\text{Im}$  results of Gao et al. are quite different from our findings. The  $\text{Im}$ s used in that study had a strontium level that would correspond to optimal doping in crystals. However, the  $1/\omega$  curves deviate markedly from what we observe for slightly under and overdoped samples. The authors performed an extended Drude analysis and found a strongly temperature dependent scattering rate. This is in sharp contrast to our results which would suggest a very weak temperature dependence. Based on our work, their samples should be

in the pseudogap state since they have an  $x$  value near optimal doping. Comparing these results with other systems, in particular with Tl2202, two factors suggest the possibility that the  $\text{Im}$ s may be overdoped. First, their  $T_c$  was near 30 K, lower than that expected for optimal doping. Secondly, it is known that the oxygen level in  $\text{Im}$ s can vary substantially and in LSCO oxygen can have a major influence on the doping level<sup>34</sup>. On the other hand, we cannot completely rule out the possibility that all of the crystal results are affected by the polishing process, and that the  $\text{Im}$ s better represent the bulk material. It is clearly important to measure  $\text{Im}$ s where the oxygen content is controlled by selective annealing.

In conclusion, the optical data in the far-infrared region, taken on two single-layered high- $T_c$  superconductors, shows clear evidence of a pseudogap state in the scattering rate. This pseudogap state extends to higher temperatures than that observed in the multi-layered underdoped cuprates such as YBCO and BSCCO. Previously, the pseudogap state feature with  $T > T_c$  was only observed in the underdoped system. In the case of LSCO this feature can be observed in the overdoped regime at a temperature substantially above the superconducting

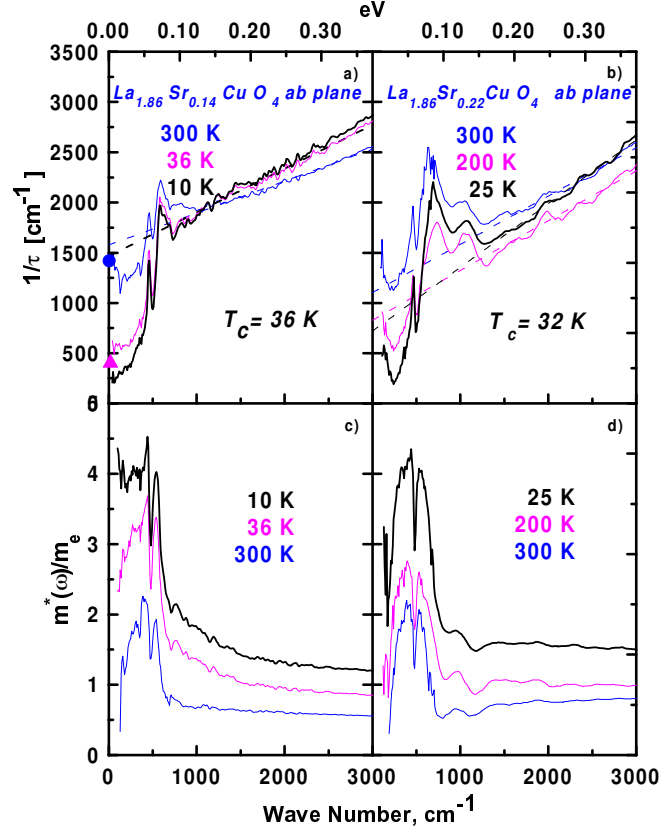


FIG. 5. Top panel: the frequency dependent scattering rate of  $\text{La}_{1.86}\text{Sr}_{0.14}\text{CuO}_4$  (a) and  $\text{La}_{1.78}\text{Sr}_{0.22}\text{CuO}_4$  (b) is calculated using Equation (1). The onset of the suppression in a conductivity corresponds to a drastic change in the frequency dependence of the scattering rate. Above  $700\text{ cm}^{-1}$  the scattering rate is nearly temperature independent and has a linear frequency dependence in the underdoped sample and temperature dependence in the overdoped sample. The dashed lines are linear fits to the scattering rate above  $700\text{ cm}^{-1}$ . Below this frequency the scattering rate varies as  $\omega^{1+}$  and shows a strong temperature dependence. Points on  $1/\tau$ -axis (a) at  $\omega=0$  corresponds to the DC-value calculated from the resistivity shown in Fig. 1. Bottom panel: The effective mass of underdoped a) and overdoped b) samples is calculated using Equation (2). The onset of enhancement of  $\frac{m^*(\omega)}{m_e}$  corresponds to the onset of the suppression of the scattering rate. The thinnest line corresponds to higher temperature.

transition temperature. This suggests that the crossover from the underdoped to the overdoped regime does not suppress  $T_c$  below  $T_c$ . The scattering rate is similar for both systems in the pseudogap state. At low frequencies,  $\omega < 700 \text{ cm}^{-1}$ , the scattering rates are temperature dependent and change with frequency in a non-linear fashion. Above  $700 \text{ cm}^{-1}$  this behaviour becomes linear. Within experimental uncertainty the observed high frequency scattering rate of the underdoped sample is not affected by temperature.

We would like to thank J.D. Garrett for help in aligning the sample and also P.C. Mason, M. Lumden and B.D. Gaulin for determining the miscut angle of the underdoped LSCO crystal. We also take this opportunity to thank K.C. Irwin and J.G. Naeini for the useful collaboration. This work was supported by the Natural Sciences and Engineering Research Council of Canada and The Canadian Institute for Advanced Research.

- <sup>1</sup> B. Batlogg, H.Y. Hwang, H. Takagi, R.J. Cava, H.L. Kao, and J. Kuo, *Physica C*, 235-240, 130 (1994).
- <sup>2</sup> H.Y. Hwang, B. Batlogg, H. Takagi, H.L. Kao, J. Kwo, R.J. Cava, and J.J. Krajewski, *Phys. Rev. Lett.*, 72, 2636 (1994).
- <sup>3</sup> S.K. Tolpygo, J.-Y. Lin, M. Givich, S.Y. Hou, and Julia M. Phillips, *Phys. Rev. B*, 53, 12454 (1996).
- <sup>4</sup> A.J. Millis and H. Monien, *Phys. Rev. Lett.*, 70, 2810 (1993).
- <sup>5</sup> D.S. Marshall, A.G. Loeser, Z.-X. Chen, and D.S. Dessau, *Physica C*, 263, 208 (1999).
- <sup>6</sup> J.W. Loram, K.A. Mirza, J.R. Cooper, and W.Y. Liang, *Phys. Rev. Lett.*, 71, 1740 (1993).
- <sup>7</sup> D.N. Basov, R. Liang, B. Dabrowski, D.A. Bonn, W.N. Hardy, and T. Timusk, *Phys. Rev. Lett.*, 77, 4090 (1996).
- <sup>8</sup> A.V. Puchkov, P. Fournier, D.N. Basov, T. Timusk, A. Kapitulnik, and N.N. Kolesnikov, *Phys. Rev. Lett.*, 77, 3212 (1996).
- <sup>9</sup> A.V. Puchkov, P. Fournier, T. Timusk, and N.N. Kolesnikov, *Phys. Rev. Lett.*, 77, 1853 (1996).
- <sup>10</sup> C.C. Homes, T. Timusk, R. Liang, D.A. Bonn, and W.N. Hardy, *Phys. Rev. Lett.*, 71, 1645 (1993).
- <sup>11</sup> D.N. Basov, R. Liang, B. Dabrowski, D.A. Bonn and W.N. Hardy, *Phys. Rev. B*, 52, R13141 (1995).
- <sup>12</sup> S. Uchida, K. Tamasaky, and S. Tajima, *Phys. Rev. B*, 53, 14558 (1996).
- <sup>13</sup> T.E. Mason, G. Aeppli, and H.A. Mook, *Phys. Rev. Lett.*, 68, 1414 (1992).
- <sup>14</sup> S. Uchida, I. Ido, H. Takagi, T. Arima, Y. Tokura, and S. Tajima, *Phys. Rev. B*, 43, 7942 (1991).
- <sup>15</sup> M.A. Quijada, D.B. Tanner, F.C. Chou, D.C. Johnston and S.-W. Cheong, *Phys. Rev. B*, 52, 15485 (1995).
- <sup>16</sup> F. Gao, D.B. Romero, B.D. Tanner, J. Talvacchio, and

- M.G. Forrester, *Phys. Rev. B*, 47, 1036 (1993).
- <sup>17</sup> W.G. Otze and P.W. Lee, *Phys. Rev. B*, 6, 1226 (1972).
- <sup>18</sup> P.B. Allen, *Phys. Rev. B*, 3, 305 (1971).
- <sup>19</sup> A. Gold, S.J. Allen, B.A. Wilson and D.C. Tsui, *Phys. Rev. B*, 25, 3519 (1982).
- <sup>20</sup> S.-W. Cheng, G. Aeppli, T.E. Mason, H. Mook, S.M. Hayden, P.C. Canfield, Z. Fisk, K.N. Clausen, and J.L. Martinez, *Phys. Rev. Lett.*, 67, 1791 (1991).
- <sup>21</sup> T. Kimura, K. Kishio, T. Kobayashi, Y. Nakayama, N. Motohira, K. Kitazawa, and K. Yamafuji, *Physica C (Amsterdam)*, 192, 247 (1992).
- <sup>22</sup> J. Orenstein and D.H. Rapkine, *Phys. Rev. Lett.*, 60, 968 (1988).
- <sup>23</sup> S. Tajima, S. Uchida, S. Ishibashi, T. Ido and H. Takagi, T. Arima and Y. Tokura, *Physica C*, 168, 117 (1990).
- <sup>24</sup> H. Takagi, B. Batlogg, H.L. Kao, J. Kwo, R.J. Cava, J.J. Krajewski, and W.F. Peck, Jr., *Phys. Rev. Lett.*, 69, 2975 (1992).
- <sup>25</sup> G. Aeppli, R.J. Cava, E.J. Ansaldo, J.H. Brewer, S.R. Kretzschmar, G.M. Luke, D.R. Noakes, and R.F. Kiehl, *Phys. Rev. B*, 35, 7129 (1987).
- <sup>26</sup> D.B. Tanner and T. Timusk, in *Physical Properties of High Temperature Superconductors I*, edited by D.M. Ginsberg (World Scientific, Singapore, 1992), p. 363.
- <sup>27</sup> T. Timusk, D.N. Basov, C.C. Homes, A.V. Puchkov, and M. Reedyk, *Journ. of Superconductivity*, 8, 437 (1995).
- <sup>28</sup> K. Tamasaku, T. Itoh, H. Takagi, and S. Uchida, *Phys. Rev. Lett.*, 72, 3088 (1994).
- <sup>29</sup> A.V. Puchkov, D.N. Basov, and T. Timusk, *J. Phys.: Condens. Matter*, 8, 10049 (1996).
- <sup>30</sup> P.A. Lee and N. Nagaosa, *Phys. Rev. B*, 46, 5621 (1992).
- <sup>31</sup> V.J. Emery and S.A. Kivelson, *Phys. Rev. Lett.*, 74, 3253 (1995).
- <sup>32</sup> Y. Yagil and E.K.H. Salje, *Physica C*, 235-140, 1143 (1994).
- <sup>33</sup> G.A. Thomas, D.H. Rapkine, S.L. Cooper, S.-W. Cheong, A.S. Cooper, L.S. Schneemeyer, and J.V. Waszczak, *Phys. Rev. B*, 45, 2474 (1992).
- <sup>34</sup> H. Zhang, H. Sato, and G.L. Liedl, *Physica C* 234, 185, (1994).